

APPLICATION OF ELECTROMAGNETIC PROPAGATION LOGGING IN THE PERMIAN BASIN OF WEST TEXAS

M. E. Eck, ARCO Oil and Gas Company
D. E. Powell, Schlumberger Well Services

ABSTRACT

A method has recently been developed for evaluating the Delaware Mountain group of West Texas by using electromagnetic propagation, photoelectric effect, and neutron-density measurements.

The Delaware Mountain group is a series of sand-shale sequences deposited in the Delaware Basin of West Texas and Southeastern New Mexico during the Guadalupian Age. For a variety of reasons, conventional interpretation methods based on resistivity measurements have not always been definitive in these formations for distinguishing between oil and water. An interpretation technique using electromagnetic propagation data, specifically porosity derived by comparing electromagnetic propagation measurements to porosity from neutron-density logs, has been used with considerable success in identifying traditional pay zones and locating new pay zones in the Bell Canyon and Cherry Canyon formations of the Delaware Mountain group.

INTRODUCTION

The Delaware Mountain group is a series of sand-shale sequences that was deposited during the Guadalupian Age in the Delaware Basin located in Culberson, Loving, Pecos, Reeves, Ward, and Winkler Counties of West Texas and Lea and Eddy Counties of Southeastern New Mexico as shown in Fig. 1. The Delaware Mountain group is divided into the Bell Canyon, Cherry Canyon, and Brushy Canyon formations. The stratigraphic cross section in Fig. 2 shows the relative age of the sands in relation to other producing horizons in the Delaware Basin. The group is approximately 3000' thick, but the majority of the wells are completed in the top 100' of the Bell Canyon. The remaining sands have not been exploited to any great extent.

Hydrocarbon accumulation in these sands occurs primarily in stratigraphic traps and occasionally in anticlinal traps. Generally, the stratigraphic traps are caused by a decrease in reservoir porosity and permeability due to increased shaliness in the sand.

Each sand is an independent reservoir that may contain oil, gas, or water. Some wells are productive in only one or two of the sands; other wells have produced from four or more separate sands with additional possibilities not yet tested. The large amount of unexplored acreage within the Delaware Basin, coupled with the number of possible productive zones, makes the Delaware Mountain group very attractive for further oil and gas development. The lack of development to date has largely been due to unreliable log analysis.

Fig. 3 illustrates the inconsistency of conventional log analysis. This is a computer-generated computation showing three sands in the Cherry Canyon formation. All three zones look equally attractive, and each exhibits porosity well above the generally accepted cutoff of 16 porosity units (pu) and water saturations below the accepted cutoff of 65 to 70 percent. However, actual production proves Zones A and B to be water bearing and Zone C to be oil bearing.

Possible reasons for these discrepancies between the log analysis and actual production are:

1. Errors in the assumed cementation (m) and saturation (n) exponents in the water saturation equation.
2. Varying water resistivities (R_w).
3. Misinterpretation of the resistivity measurement.

The first possibility was checked using core analysis. The m and n exponents were found to be relatively close to the assumed values. The formation water resistivity was determined from analysis of offset producers to provide consistent S_w calculations. Three possible explanations for a misinterpretation of the resistivity measurements are:

1. Varying grain sizes of the sands. This would cause the irreducible bulk volume water to vary in the formation, and measured resistivity would vary accordingly.
2. Laminar streaks of carbonates interbedded in the sands causing the measured R_t to increase, possibly enough to make a water sand appear as attractive as an oil sand.
3. Clays such as illite and chlorite affecting the resistivity response.

In any case, conventional logs have proven inconsistent in selecting the productive zones, and other evaluation methods have been used to find production. Mud logging was used in some wells to pick perforations. Unfortunately, it is inconclusive; one problem is the possibility of gas kicks coming from open intervals above the zone being penetrated. Sidewall coring has been used for determining which zones contain residual oil saturation, but core recovery can be poor for various reasons. Full-diameter coring is another alternative. However, it is not economically feasible to core 3000' of sand to properly evaluate the Delaware Mountain group. For this reason, both full-diameter and sidewall cores provide only discrete sampling, which may result in unwarranted completions or missed zones.

However, coring did lead to the conclusion that determining the zones containing residual hydrocarbons would be the key to finding the productive zones. The EPT* Electromagnetic Propagation Tool was designed to measure residual when combined with other porosity devices. The obvious benefits were that it could be measured continuously, more economically, and with increased reliability compared to the other available evaluation techniques.

MEASUREMENT HARDWARE

The EPT tool makes its measurements using four microwave antennas placed in an antenna block on the sonde body as shown in Fig. 4. This configuration is similar to the transducer array used in the Borehole Compensated sonic tool, and it helps eliminate errors associated with varying mudcake thickness, pad tilt, and minor electronic imbalances. The two transmitters are alternately pulsed to radiate a 1.1-GHz electromagnetic wave of a known magnitude into the formation. The microwave will travel through the formation and then be picked up by two receiving antennas which are a known distance apart. In this manner the EPT tool measures the travel time and the attenuation rate of the electromagnetic wave between the two receivers.

*Mark of Schlumberger

INTERPRETATION

Table 1 is a listing of the propagation times of common reservoir rocks and fluids. Note the significant difference between the travel time (t_{p1}) of water and the t_{p1} of oil or gas. This forms the basis for the calculation of an EPT-derived bulk volume of water in the flushed zone, independent of water and formation resistivities and Archie's equation. Thus, the EPT tool responds primarily to the bulk volume of water, which is the water-filled porosity in the formation. When the bulk volume of water (ϕ_{EPT}) is compared to the matrix porosity measured by the Litho-Density* (LDT) and CNL* Compensated Neutron tools, the difference is the volume of residual hydrocarbons present.

Two techniques have been developed for the computation of EPT porosity. These are the " t_{po} method" and the "complex refractive index method" (CRIM). The CRIM technique has been discussed in previous papers.¹ The t_{po} method of computing ϕ_{EPT} from measured t_{p1} and attenuation is currently being used in wellsite computations. An in-depth derivation of this method has been presented in previous publications.² Only the equations of immediate importance to this paper will be repeated here.

Initially, conductivity losses are removed from the travel time t_{p1} using the equation:

$$t_{po} = (t_{p1}^2 - \frac{A_c^2}{3604})^{1/2}, \quad (1)$$

where

t_{po} = loss-free travel time

t_{p1} = travel time from log

A_c = corrected attenuation

Using a weighted-average model and assuming $S_w = 100$ percent, we get

$$t_{po} = \phi_{EPT} t_{pwo} + (1 - \phi_{EPT}) t_{pma} \quad (2)$$

Solving for ϕ_{EPT} ,

$$\phi_{EPT} = \frac{t_{po} - t_{pma}}{t_{pwo} - t_{pma}}, \quad (3)$$

where

ϕ_{EPT} = the water-filled porosity from EPT tool

t_{pwo} = the loss-free propagation time of the water

t_{pma} = the loss-free propagation time of the matrix

The propagation time of water varies with the temperature and is calculated using Eq. 4.

$$t_{pwo} = 20 \left(\frac{710 - ^\circ F/3}{444 + ^\circ F/3} \right) \quad (4)$$

The propagation time of the matrix varies with lithology. There are three methods of deriving t_{pma} , depending on formation lithology and the other logs available on the

well. This is a critical value so the method must be chosen carefully. These methods are outlined in other literature.³ The method used in the examples is summarized here.

Three-Mineral Model

When the lithology is complex and continually changing, it is necessary to use a three-mineral model to compute t_{pma} . This technique requires the combination LDT-CNL log. The ρ_b , ϕ_N , and P_e measurements are combined to compute the apparent grain density and the apparent matrix volumetric cross section. These values are then entered into the model shown in Fig. 5 to find the percentages of three rock types (P_1 , P_2 , P_3) in the matrix. Each rock type in the model has its characteristic t_{pma} as shown in Table 1. Then, the t_{pma} of the composite matrix is given by:

$$t_{pma} = (P_1) (t_{pm1}) + P_2 (t_{pm2}) + P_3 (t_{pm3}), \quad (5)$$

where

P_1 = fraction of limestone

P_2 = fraction of sandstone

P_3 = fraction of shale and/or dolomite

It has been found that most Delaware sands contain four basic rock types: sandstone, limestone, dolomite, and shale. Presently, the field interpretation technique is limited to a three-rock interpretation. Therefore, to account for a fourth rock type, the t_{pma} of dolomite can be assigned to t_{pm3} , in essence negating the effects of bound water in the shales. Comparing ϕ_{EPT} with effective porosity (ϕ_e), the net result remains residual hydrocarbon bulk volume. This approach has proven very effective in the handling of four rock types without losing the ability to detect hydrocarbons. This model is used in the following examples.

LOG EXAMPLES

Example 1

Fig. 6 shows the DLL*/MSFL and LDT/CNL logs run over a section of the Cherry Canyon sand in Culberson County, Texas. In this example there are three sands present. All three look equally attractive in the computer analysis of the conventional logs shown in Fig. 2. Extensive testing of offset wells showed Zones A and B contain mostly water and Zone C is the oil-bearing sand.

Fig. 7 shows a playback of ϕ_e from LDT/CNL data and ϕ_{EPT} . Clearly, Zones A and B are water filled and Zone C contains residual hydrocarbons.

The well was perforated in Zone C, treated with acid, and fractured to increase permeability. It is believed that the treatment broke into Zone B and caused the high water cut. The well is producing 30 BOPD, 180 BWP, and 35 Mcfg/D.

Example 2

Fig. 8 shows the DLL/MSFL and LDT/CNL logs run over a section of Cherry Canyon sand in Reeves County, Texas. Using standard log analysis, Zone A has a lower S_w than Zone B. Resistivity profiles also indicate that Zone A is probably hydrocarbon bearing and Zone B is water bearing. The left side of Track 2 is the residual oil

saturation plotted from the analysis of full-diameter cores. Core data shows Zone A is 100 percent water bearing and Zone B contains residual hydrocarbons, which is opposite of conventional analysis.

Fig. 9 shows the ϕ_{EPT} vs ϕ_e overlay log of this interval. Separation between the curves indicates Zone A contains water and Zone B contains oil. This well was completed in Zone B flowing 139 BOPD, 157 BWP, and 125 Mcfg/D. The agreement of the EPT evaluation and full core data is impressive, especially in light of the contradictory results obtained from conventional log analysis.

Example 3

Fig. 10 shows the DLL and LDT/CNL logs for a Cherry Canyon well in Ward County, Texas. In this particular section there are six sands with porosities of 20 pu or greater. Using conventional interpretation techniques to calculate water saturation, Zones B and C appear to contain hydrocarbons. Zone C was the primary objective in this well.

Fig. 11 is the ϕ_{EPT} vs ϕ_e interpretation for this well. Note that the curves overlay in Zones A, B, D, and F, but in Zones C and E the curves show separation indicating residual hydrocarbons. Zone E was untested in the area, and sidewall cores indicated all water; i.e., no fluorescence and no odor. This was a case where hydrocarbons were seen with the EPT overlay but not with resistivity logs or sidewall cores.

The well was completed in Zone E and is now flowing 150 BOPD, 20 BWP, and 700 Mcfg/D, making it one of the highest producers in the area. Zone C is still behind pipe and has excellent plugback potential.

Example 4

Fig. 12 shows the DLL/MSFL and LDT/CNL logs run through the Ramsey sand and Lamar lime section of a Bell Canyon well in Winkler County, Texas. The DLL/MSFL log was run first. Because of discouraging hydrocarbon indication from the resistivity logs and the well's low structural position to other offsets, the operator planned to plug the well. However, he finished logging and observed a slight gas effect present on the LDT/CNL log. This could have been interpreted as a clean sand. However, with the additional information provided by the EPT log (Fig. 13), the LDT/CNL crossover was interpreted as gas. The decision was made to run pipe because the ϕ_{EPT} vs ϕ_e overlay confirmed hydrocarbons. The well was completed in the zone indicated and is now producing 600 Mcfg/D water free.

CONCLUSIONS

For the first time, accurate evaluation of the Delaware Mountain group from logging tools is available. This new logging technique has proven to be equally effective and consistent in these sands throughout the Delaware basin. The ϕ_{EPT} vs ϕ_e overlay eliminates the inconsistencies associated with the use of resistivity tools. It does not require a knowledge of the formation water resistivity, and it performs well in the salt muds normally used in the Delaware Basin.

This technique provides the operator with an onsite evaluation of the Delaware Mountain group. The tool's response has shown close agreement with residual oil saturation data from full-diameter cores, which is the key to finding productive zones. Thus, the ability has been found to identify traditional pay zones and to find new pay zones when traditional methods fail.

In summary, the Delaware Mountain group can now be exploited more effectively and more economically. The EPT tool provides reliable, accurate data not available previously from conventional log analysis.

NOMENCLATURE

A_c	Corrected attenuation
BOPD	Barrels of oil per day
BWPD	Barrels of water per day
DLL	Dual Laterolog
DPHI	Density porosity
EMCP	EPT matrix-corrected porosity
GHz	Billion cycles per second
LLD	Deep resistivity
LLS	Shallow resistivity
m	Cementation exponent
Mcfg/D	Thousand cubic feet of gas per day
MSFL	Microspherically Focused log
n	Saturation exponent
NPHI	Neutron porosity
P_1	Fraction of limestone
P_2	Fraction of sandstone
P_3	Fraction of shale or dolomite
P_e	Photoelectric absorption cross section index
PEF	Photoelectric absorption cross section index
PHIE	Effective porosity
ϕ_e	Effective porosity
ϕ_{EPT}	Water-filled porosity from EPT log
ϕ_N	Porosity from Compensated Neutron log
b	Bulk density
R_t	True formation resistivity
R_w	Connate water resistivity
S_w	Water saturation
t_{p1}	Microwave travel time
t_{pm1}	t_{pma} of limestone
t_{pm2}	t_{pma} of sandstone
t_{pm3}	t_{pma} of dolomite and/or shale
t_{pma}	Loss-free travel time of the matrix
t_{po}	Loss-free travel time
t_{pwo}	Loss-free travel time of water

REFERENCES

1. Wharton, R. P.; Hazen, G. A.; Rau, R. N.; and Best, D. L.: "Electromagnetic Propagation Logging: Advances in Technique and Interpretation," paper SPE 9267 presented at the SPE 55th Annual Technical Conference and Exhibition, Dallas, September 1980.
2. Wharton, R. P. and Delano, J. M., Jr.: "An EPT Interpretation Procedure and Application in Fresh Water, Shaly, Oil Sands," paper E presented at the SPWLA 22nd Annual Logging Symposium, Corpus Christi, Texas, June 1981.
3. Gardner, J. S. and Dumanoir, J. L.: "Litho-Density Log Interpretation," paper N presented at SPWLA 21st Annual Logging Symposium, Lafayette, Louisiana, 1980.

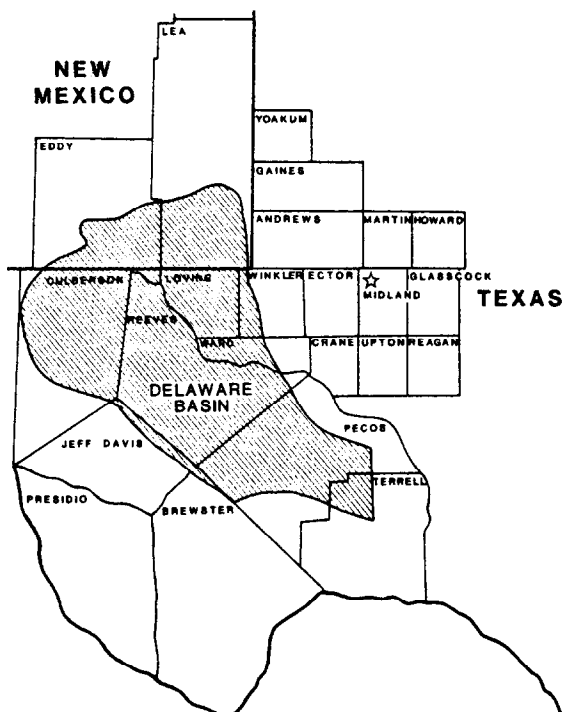


Figure 1 - Map of Delaware basin in west Texas and southeastern New Mexico

SYSTEM	SERIES	DELAWARE BASIN
PERMIAN	OCNOA	DEWEY LAKE RUSTLER SALADO CASTILE
	GUADALUPE	DELAWARE MT GROUP: BELL CANYON CHERRY CANYON BRUSHY CANYON
	LEONARD	BOHE SPRING
	WOLFCAMP	WOLFCAMP
PENNSYLVANIAN	YIRGIL	(ABSENT OR THIN)
	MISSOURI	
	DES MOINES	STRAWN
	ATOKA	ATOKA
	MORROW	MORROW
MISSISSIPPIAN	CHESTER MEREMEC OSAGE KINDERHOOK	CHESTER MEREMEC - ^{BARNETT} OSAGE KINDERHOOK WOODFORD
		DEVONIAN
SILURIAN		MID. SILURIAN FUSSELMAN
ORDOVICIAN	UPPER	STYLAN MONTOLA
	MIDDLE	SIMPSON
	LOWER	EILLENBURGER
CAMBRIAN	UPPER	CAMBRIAN
PRECAMBRIAN		

Figure 2 - Delaware basin stratigraphic cross section

RELATIVE PROPAGATION TIMES FOR VARIOUS SUBSTANCES AT 1.1 GHZ

SUBSTANCE	t _p (ns/m)
Sandstone	7.2
Dolomite	8.7
Limestone	9.1-10.2
Anhydrite	8.4
Dry Colloids*	8.0
Halite*	7.9-8.4
Gypsum*	6.8
Oil	4.7-5.2
Gas or Air	3.3
Shale	7.45-16.6
Fresh Water at 25°C	28.0

*Values estimated from published literature.

COMPUTER PROCESSED LOG

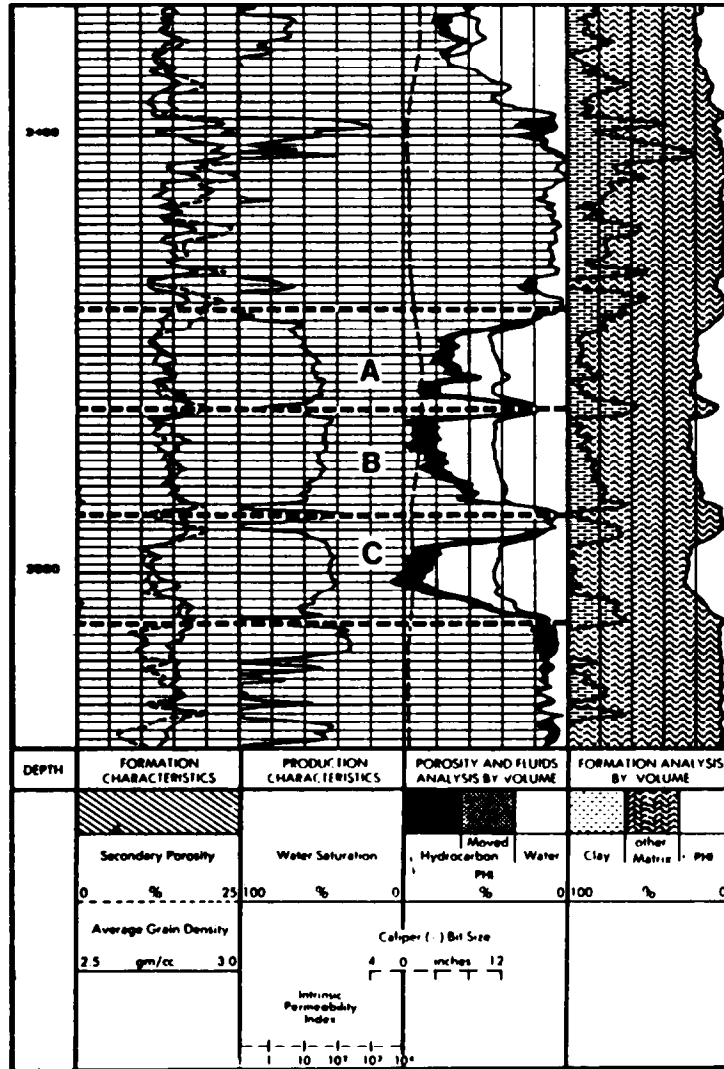


Figure 3 - Log computed using openhole data from Cherry Canyon well in Culberson County, Tx.

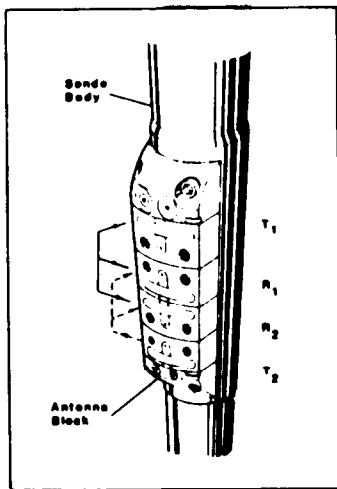


Figure 4 - EPT antenna configuration

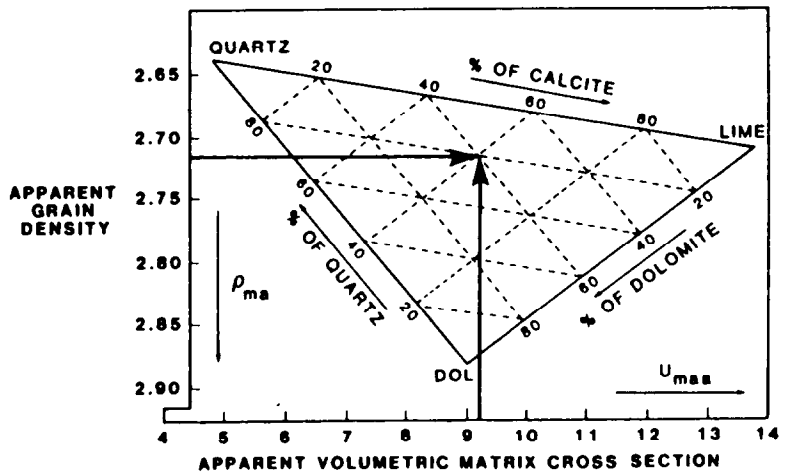


Figure 5 - LDT three-mineral model

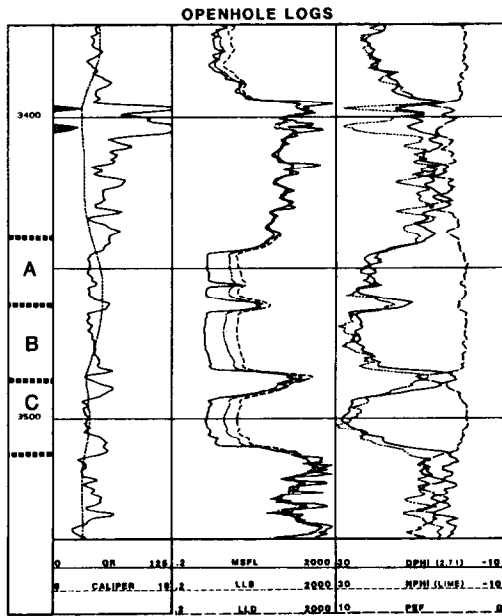


Figure 6 - Openhole logs from Cherry Canyon well in Culberson County, Tx.

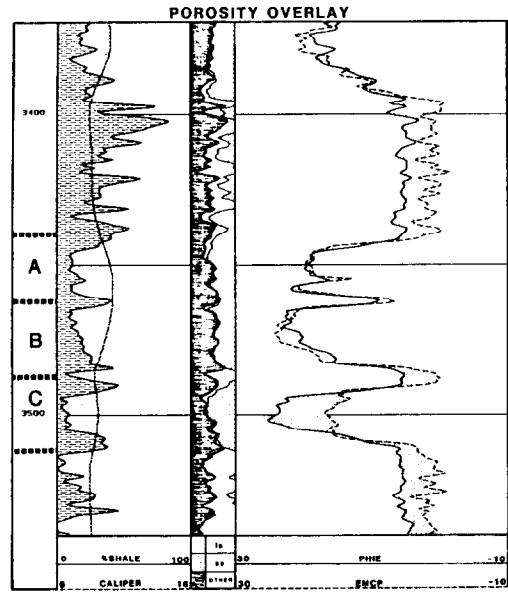


Figure 7 - ϕ_{EPT} vs. ϕ_{θ} overlay from Cherry Canyon well in Culberson County, Tx.

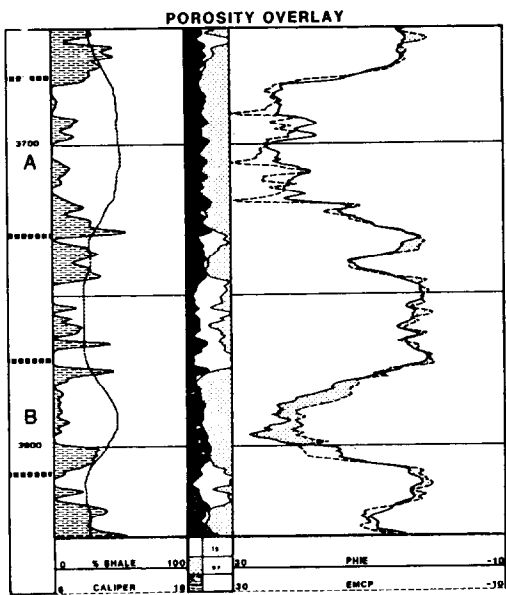


Figure 8 - Openhole logs from Cherry Canyon well in Reeves County, Tx.

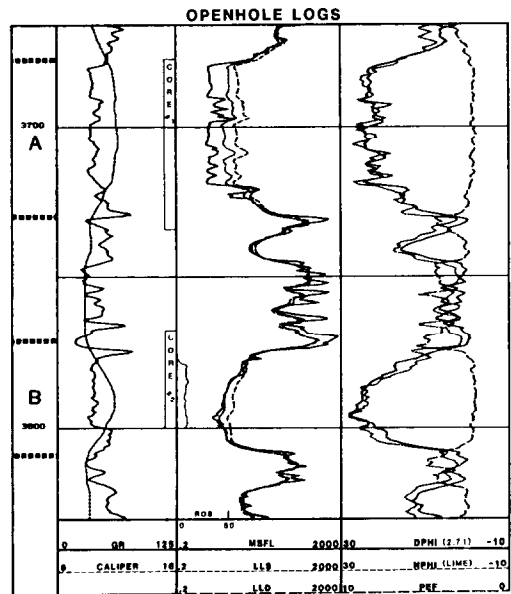


Figure 9 - ϕ_{EPT} vs. ϕ_{θ} overlay from Cherry Canyon well in Reeves County, Tx.

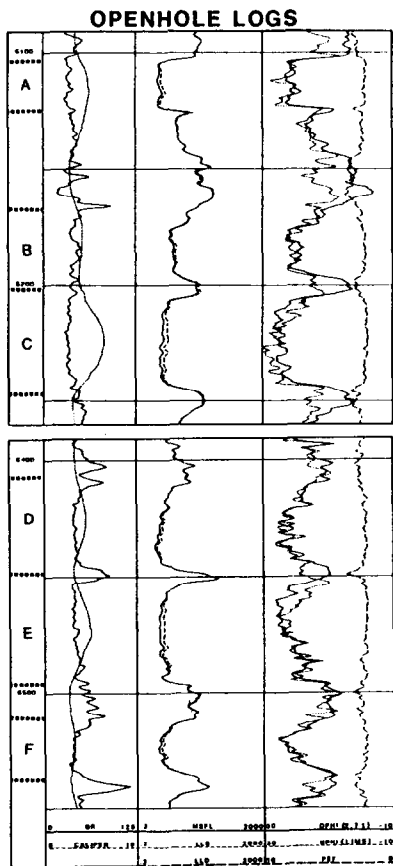


Figure 10 - Openhole logs from Cherry Canyon well in Ward County, Tx.

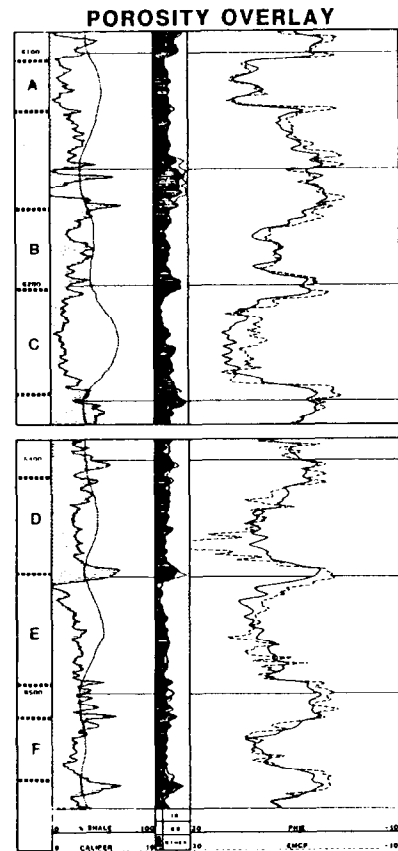


Figure 11 - ϕ_{EPT} vs. ϕ_o overlay from Cherry Canyon well in Ward County, Tx.

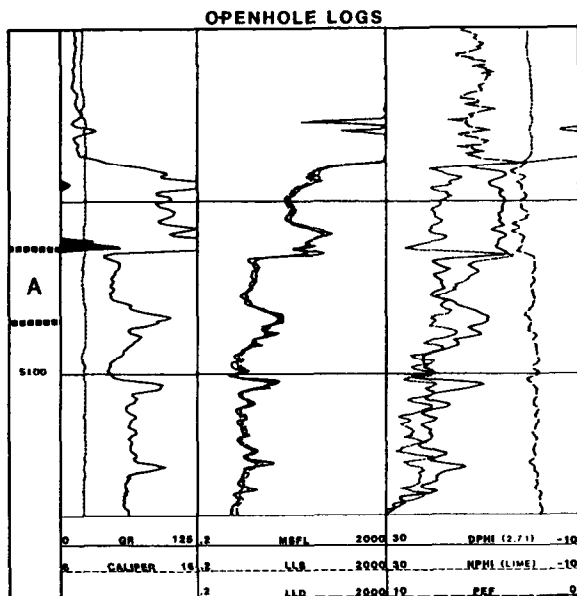


Figure 12 - Openhole logs from Bell Canyon well in Winkler County, Tx.

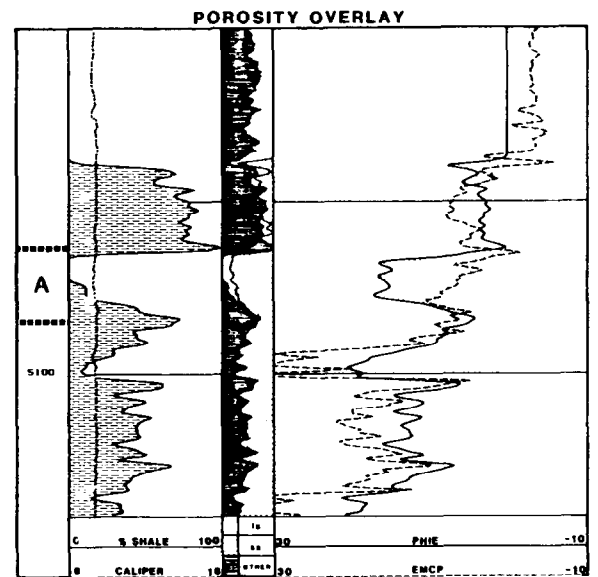


Figure 13 - ϕ_{EPT} vs. ϕ_o overlay from Bell Canyon well in Winkler County, Tx.